CO_2 profiling by space-borne Raman lidar

ISTP 2019, Toulouse, 20-24 May 19

Paolo Di Girolamo[1], Volker Wulfmeyer[2], Andreas Behrendt[2], Carmine Serio[1], Davide Dionisi[3]

[1]Scuola di Ingegneria, Università della Basilicata, Potenza, Italia
[2]Institut fuer Physik und Meteorologie, Universitaet Hohenheim, Stuttgart, Germany
[3]ISMAR-CNR, Roma, Italy

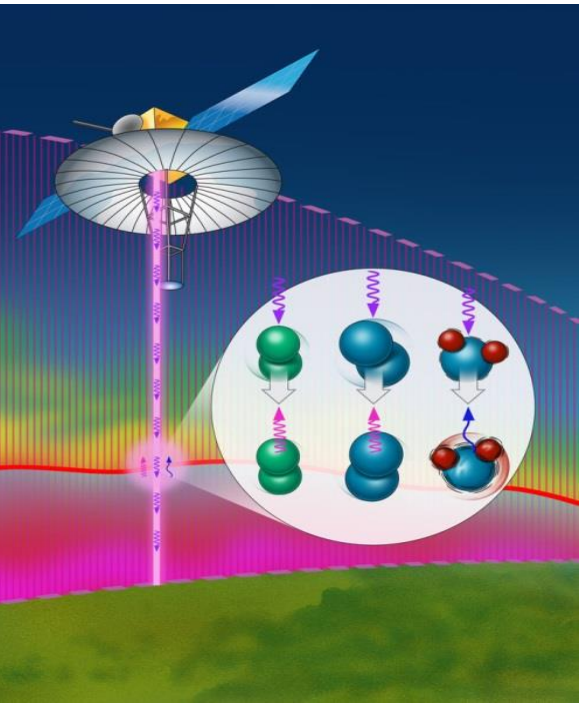

Motivation

- CO_2 mixing ratio in the atmosphere has substantially increased from values around 300 ppm in the fifties of previous century to a current value of 415-420 ppm, with an annual increasing rate of approximately 2 ppm.
- Approximately 50 % of CO_2 amount produced through fossil fuel combustion and other human activities is injected in the atmosphere and accumulates in it, while the remaining 50 % is absorbed by the oceans and the terrestrial biosphere.
- Forests cover ~30% of the Earth's global land area and store large amounts of carbon captured from the atmosphere.

- In order to properly quantify this sink mechanism and its contribution to the carbon cycle, accurate measurements of the CO_2 gradients between the forest floor and the top of the canopy, and their temporal variations, are urgently needed.

- This ultimately translates into the capability to perform accurate and high vertical and horizontal resolution measurements of CO_2 mixing ratio profiles.

Although the space and ground network for CO_2 monitoring has regularly expanded over the past 50 years, it does not guarantee the necessary spatial and temporal resolution needed for a quantitative analysis of sources and sinks.

Space sensors provide CO_2 measurements above forest canopies, which do not allow to properly estimate Gross Primary Production (GPP).

These observational gaps could be addressed with an active remote sensing system in space based on the roto-vibrational Raman lidar technique.

Raman lidar technique for CO_2 profiling

Despite its important potential scientific impact, the CO_2 vibrational Raman lidar technique has received limited attention in the last 25 years both at theoretical and experimental level, mainly because of the limited precision that this technique could guarantee, due to the limited cross-sections and to the low concentration of the sounded species.

However, in the last decade, considerable technological progress has been achieved in the design and development of solid-state laser sources with high optical power, large-aperture telescopes and high-gain and quantum efficiency detectors.

This technological progress allows today reaching a new level of performance in the Raman lidar measurements of CO_2.

In a Raman system, CO_2 profile measurements are possible, together with simultaneous measurements of the temperature and water vapour mixing ratio profile and a variety of additional variables (aerosol backscatter and extinction profiles, PBL depth, cloud top and base heights, cloud optical depth).

Observational requirements for CO_2 profiling

In order to properly design and size a Space Raman lidar, observational requirements have to be assessed and defined.

Vertical variability in CO_2

Seasonal and annual mean of CO_2 vertical profiles reflect the combined influences of surface fluxes and atmospheric mixing.

During the **summer** in the Northern Hemisphere, atmospheric CO_2 concentrations are generally **lower** near the surface than in the free troposphere, reflecting the greater impact of **terrestrial photosynthesis** over **industrial emissions** at this time (Stephens et al., 2007).

Conversely, during the **winter**, **respiration** and **fossil-fuel sources** lead to high **low-altitude** atmospheric CO_2 concentrations at northern locations. The gradients are comparable in magnitude in the two seasons, this being of the order of **10 ppm**.

CO_2 gradients between the forest floor and the top of the canopy are in the range **75-100 ppm** in daytime and **10-50 ppm** at night. Both ranges represented spring conditions when canopy leaf area development is not completed.

The Space Raman lidar has to be designed and sized with the goal of allowing measurements of these gradients.

- Vertical resolution: 200 m
- Horizontal resolution : 50 km
- Accuracy: 2-5 ppm

Mission Characteristics

The lidar setup considered in the present research effort heavily relies on the mission concept of ATLAS proposed to the European Space Agency in response to the Call for Explorer-10 Mission Ideas. Simulations consider a sun-synchronous low Earth orbit, with an orbiting height and speed of 450 km and 7 km/s, respectively. A dawn-dusk orbit with overpasses at 6/18 h local time has been selected for the simulations.

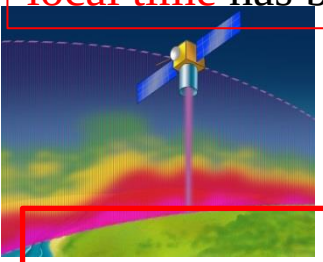

Instrumental concept benefits from recent advances in solid-state laser, large-aperture telescope, and detector technologies.

Transmitter

- frequency-tripled diode-laser pumped Nd:YAG laser
- average power of 250 W at 355 nm
- new generation of pump chambers and diode lasers (demon. under dev. at UHOH)
- electrical-to-optical efficiency > 5 % (by improving power supply and diode laser efficiencies, reducing electrical losses, optimizing pump chambers and the laser conversion efficiency).
- Inclusion of several amplification stages (3-4), each one embedding high-density stacks of pumping diodes
- Use of diode laser pumping determines radiative cooling to be sufficient.
- Far less complex than, e.g., for ADM or EarthCARE.

Does not require:
- ➢ frequency stabilization unit,
- ➢ beam shaping optics,
- ➢ specific operational modes (repet. rates and bursts).

Slab amplifiers with single pulse energies of 12 J (5 times higher) were demonstrated in Liu et al. (2017). A pulse energy >100 J in Mason et al. (2017) .

Mission Characteristics

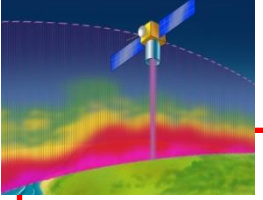

Receiver

- large-aperture, lightweight telescope, 4 m diameter
- Different technological solution:
  - rigid primary mirror (single physical element or segmented optics),
  - Rigid central mirror with folded deployable outer sections
  - inflatable optics
- several glass materials (e.g. Zerodur, SiC, etc.) with appropriate low weight and thermal stability properties for this type of space application
- no astronomical quality needed (no diffraction-limited performances (swe<λ/14), surface wavefront error< λ RMS)

Large aperture primary mirrors (with a total surface of ~ 10 m^2), with adequate rigidity, low weight (primary mirror areal density ~ 15 kg/m^2), high wave-front quality (< λ/3) and sufficient temporal and thermal stability, have been demonstrated (Mazzinghi *et al.*, 2006) to be developable based on the use of segmented mirrors, including a very rigid carbon-fibre composite back-plane and a thin Zerodur glass shell, supported by a set of high efficiency electromagnetic, actively-controlled actuators [102].

- receiving field-of-view = 25 μrad

- In the present mission concept, the Raman lidar collects five primary lidar signals:
  - CO_2 vibrational Raman signal $P_{CO_2}(z)$
  - water vapour roto-vibrational Raman signal $P_{H_2O}(z)$
  - O_2-N_2 high- and low-quantum number rotational Raman signals $P_{loJ}(z)$ & $P_{HiJ}(z)$
  - elastic backscatter signal @ λ_0 $P_{\lambda_0}(z)$

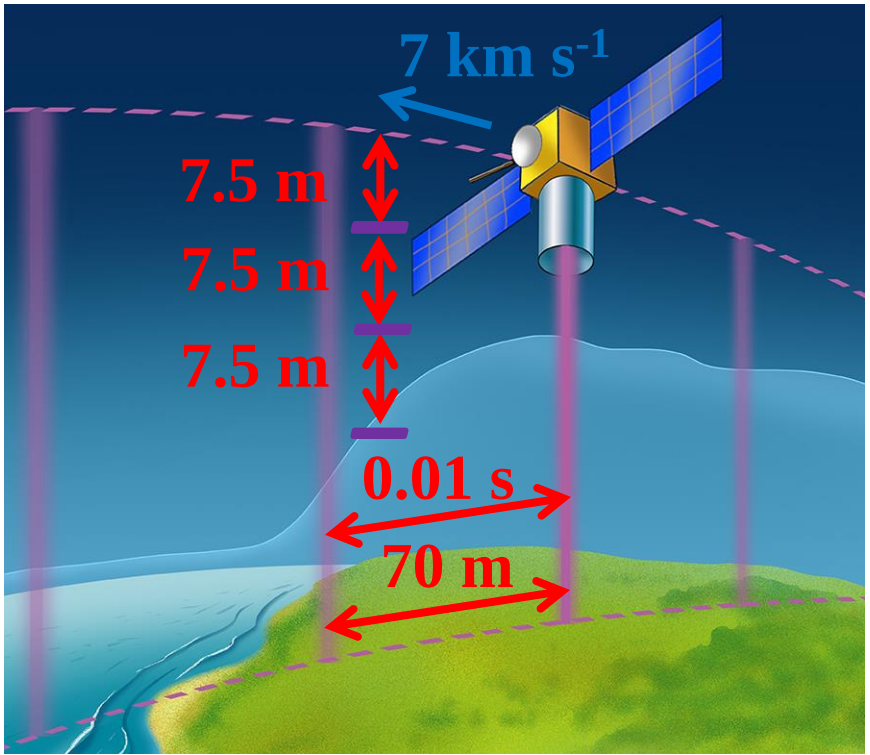

Horizontal and vertical signal averaging to reduce signal statistical uncertainties.

Vertical resolution → Δz=200 m

Horizontal resolution → Δh=50 km

obtained with an time integration of 7.14 s

An **Input CO_2 mixing ratio profile data for the Simulator** was generated which accounts **for different vertical gradients** associated with the conflicting contributions of **terrestrial photosynthesis** and **industrial emissions**, and **CO_2 capturing within forest canopy**. This input profile includes a :

- **10 ppm** increase at an **altitude of 2 km** from a value of **400 ppm** to one of **410 ppm**, introduced in order to simulate the daytime CO_2 depletion taking place within the mixed layer. In addition to this;
- **50 ppm** decrease is considered at an **altitude of 50 m above the surface level**, which is intended to represent CO_2 capturing within forest canopy.
- Other atmospheric quantities considered in the simulation include:
  - vertical profiles of pressure, temperature, and humidity from the U.S. Standard Atmosphere 1976 atmospheric reference model;
  - Aerosol optical properties from the median aerosol extinction data from the ESA ARMA Model.

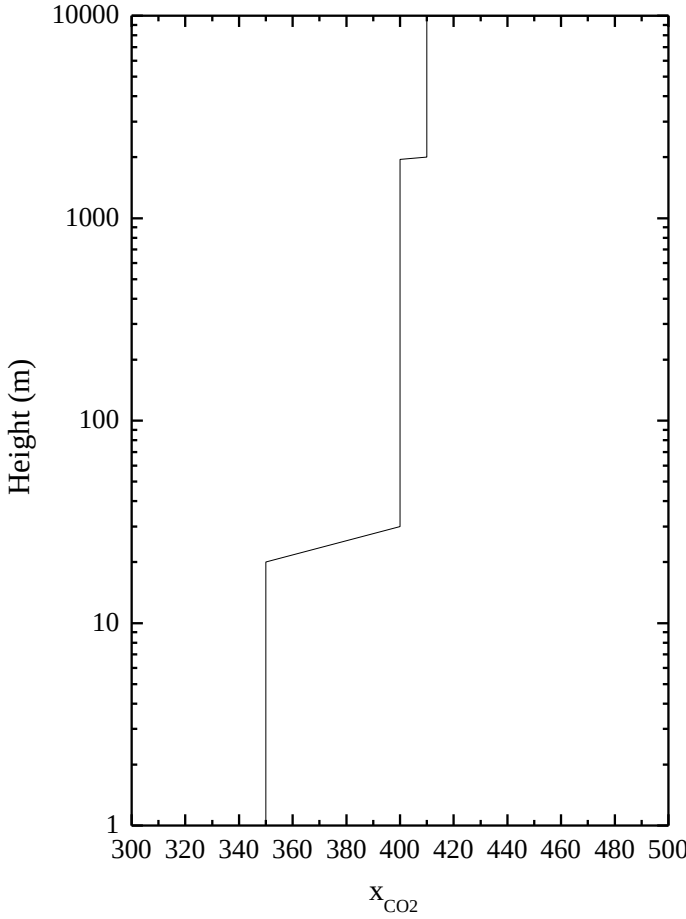

The Space Raman lidar has to be designed and sized with the goal of perfomimg measurements allowing to resolve these gradients.

- Vertical resolution: 200 m
- Horizontal resolution : 50 km
- Accuracy: 2-5 ppm

Simulation results

An assessment of the expected system performance has been performed based on the application of an analytical simulation model developed at University of Basilicata.

Considering a vertical and horizontal resolution of 200 m and 50 km, respectively, the statistical uncertainty (precision) affecting CO_2 mixing ratio profile measurements is not exceeding **5 ppm** at night and **60 ppm** in daytime from the surface up to an **altitude of 5 km**.

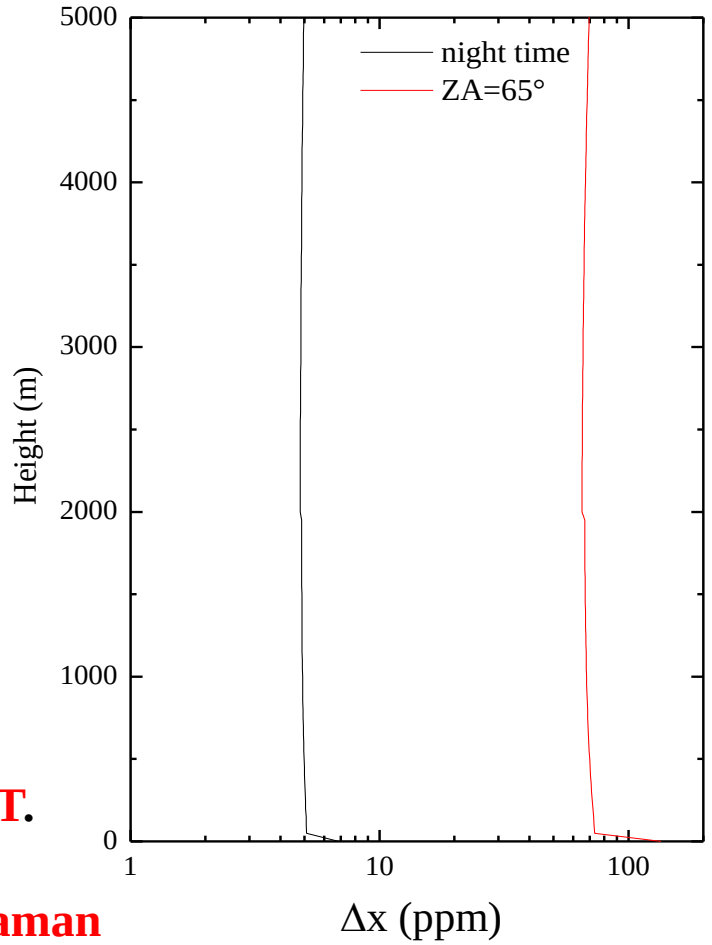

Night-time performance is acceptable, but daytime is **NOT.**

However, so far we have been exploiting only the Raman signal in the anti-Stokes $2v_2$ vibrational band.

CO_2 Spectroscopy

Fermi resonance results in the splitting of two vibrational bands that have nearly the same energy and symmetry in both IR and Raman spectroscopies. The two bands are usually a fundamental vibration and either an overtone or combination band.

As a result, two strong bands are observed in the spectrum, instead of the expected strong and weak bands. It is not possible to determine the contribution from each vibration because of the resulting mixed wave function.

The three fundamental vibrations of CO_2 are ν_1= 1337 cm^{-1}, ν_2=667 cm^{-1}, ν_3=2349 cm^{-1}.

As a result of Fermi resonance, two strong bands are present, with frequencies ν_1=1337 cm^{-1} and $2\nu_2$(2 x 667 cm^{-1})=1334 cm^{-1}.

Stokes branch

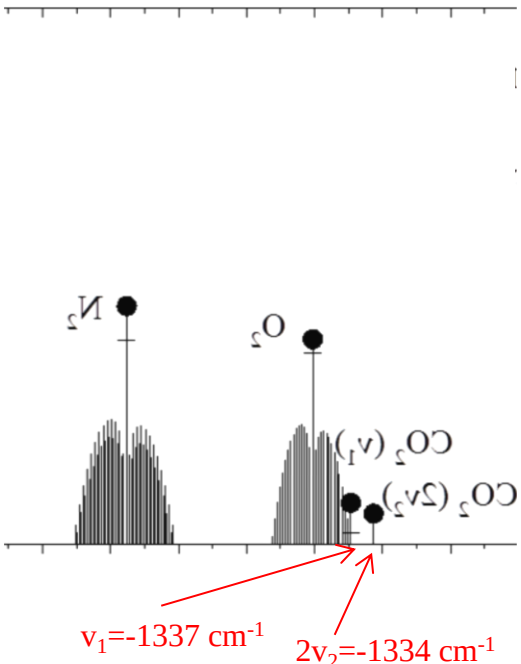

Anti-Stokes branch

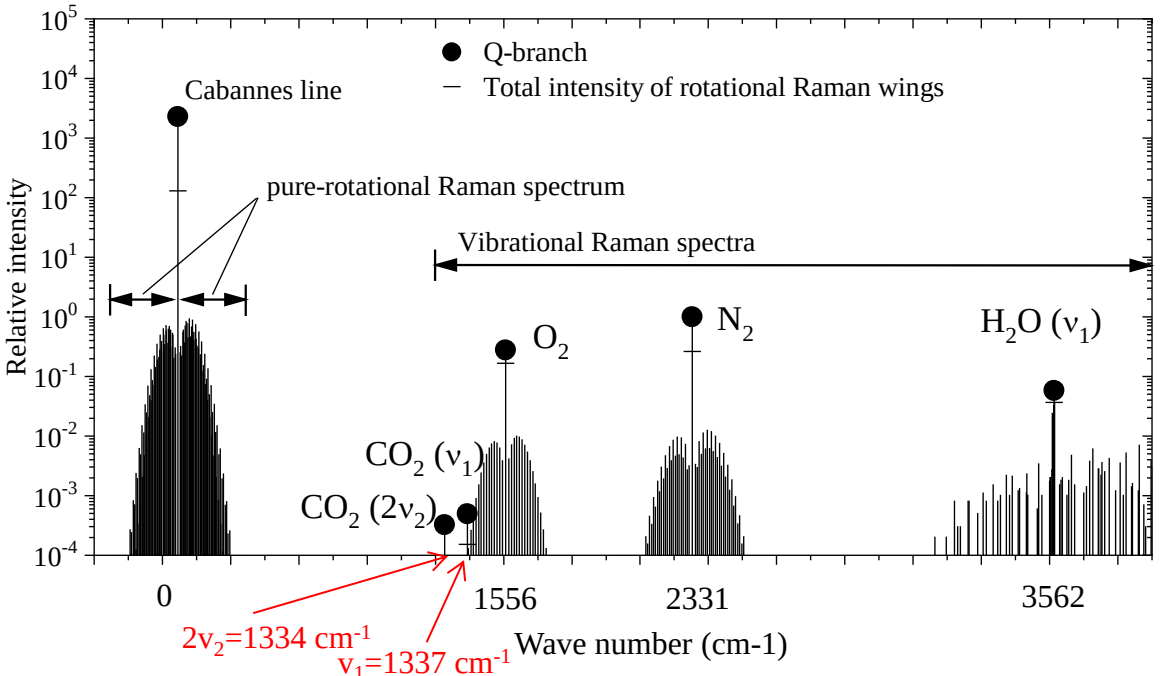

Thus, measuring the Raman lidar echoes from the two bands v_1 and $2v_2$ both in the Stokes and anti-Stokes branches, the intensity of the CO_2 Raman lidar signal can be increased by a factor of 4 to 5.

This solution can be implemented in combination with a reduction of the receiving field-of-view from 25 μrad to 10 μrad.

This traslates into a statistical uncertainty (precision) affecting CO_2 mixing ratio profile measurements not exceeding **0.5 ppm** at night and **5 ppm** in daytime from the surface up to an **altitude of 5 km**.

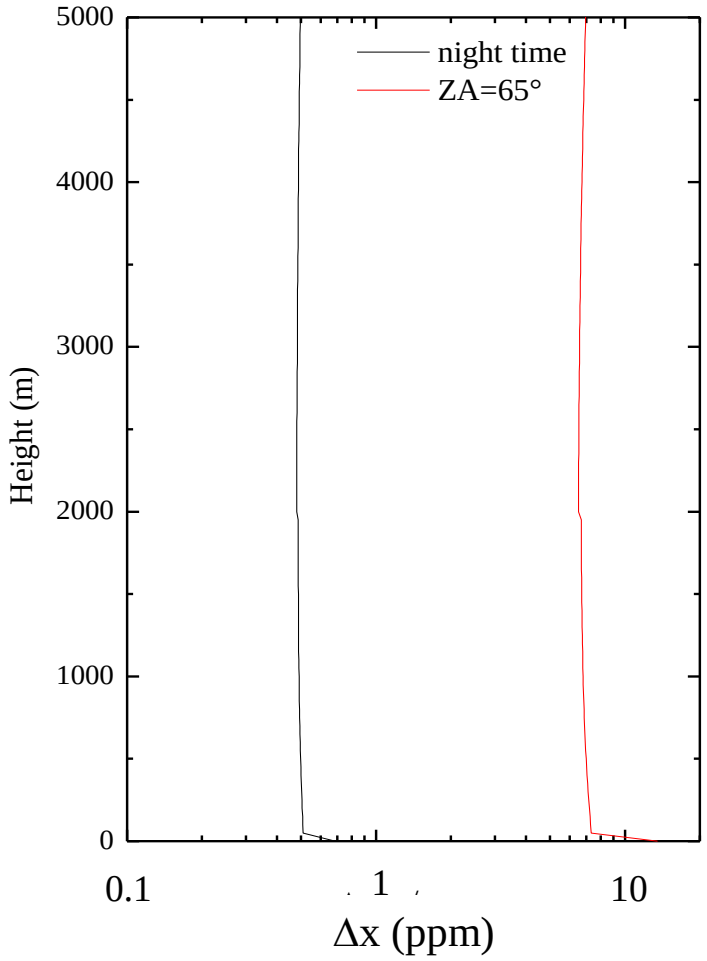

Measured parameters/expected perform

Clear-sky conditions

Accuracy estimated with experimentally-validated performance model (Di G

Variable	Resolution (vertical/horizontal)	Precision
Water vapor mixing ratio	200 m / 50 km	**2-20 %**
Temperature	200 m / 50 km	**0.4-0.75 K**
Relative humidity	200 m / 50 km	2-20 %
Planetary boundary layer height	100 m / 5 km	100 m
Particle backscatter & extinction	50-100 m / 10-50 km	1-3 % & 3-20 %
	50-100 m / 5 km	50-100 m
	50 km	5 %

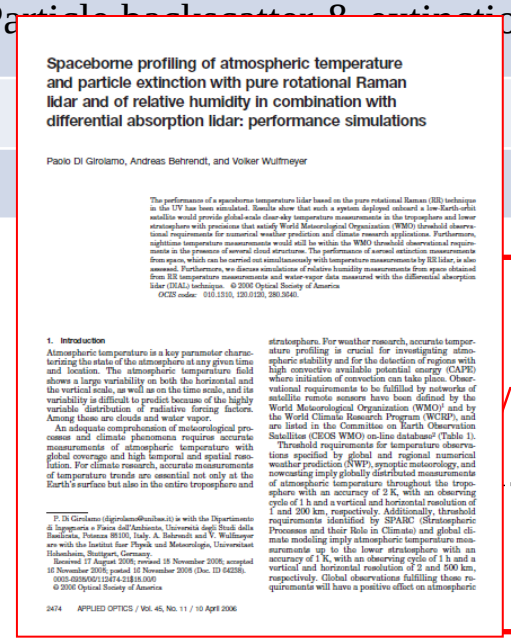
Spaceborne profiling of atmospheric temperature and particle extinction with pure rotational Raman lidar and of relative humidity in combination with differential absorption lidar: performance simulations

Paolo Di Girolamo, Andreas Behrendt, and Volker Wulfmeyer

1. Introduction

i.e.,
/day
200

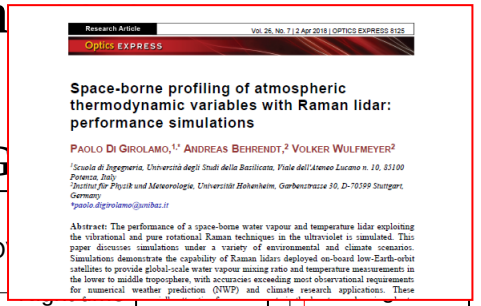
Research Article
Optics EXPRESS
Vol. 26, No. 7 | 2 Apr 2018 | OPTICS EXPRESS 8125

Space-borne profiling of atmospheric thermodynamic variables with Raman lidar: performance simulations

Paolo Di Girolamo,[1,*] Andreas Behrendt,[2] Volker Wulfmeyer[2]

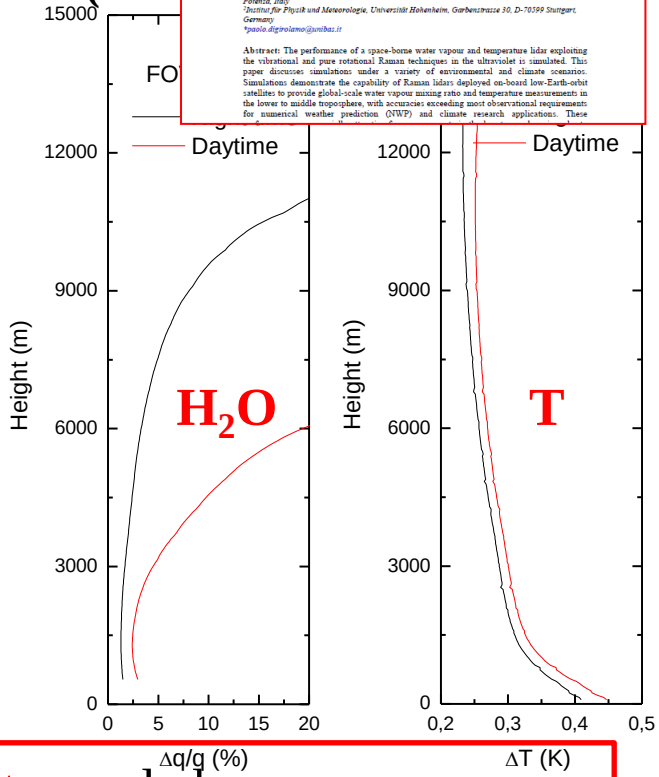

- No ancillary data needed
- Errors provided with each retrieved profile
- Clear air, above clouds, through broken clouds & through/below overcast thin clouds

Summary

- An accurate quantitative assessment of the various components of the carbon cycle requires accurate measurements of the different sources and sinks.
- For the purpose of estimating forests' carbon capturing capabilities, accurate measurements of CO_2 gradients between the forest floor and the top of the canopy are needed, which ultimately translates into the capability to measure CO_2 concentration profiles.
- Simulations reveal that a space-borne Raman lidar based on the roto-vibrational technique, if properly conceived (i.e. exploiting both v_1 and $2v_2$ vibrational bands in both the Stokes and anti-Stokes branches), may provide CO2 mixing ratio profile measurements with the level of accuracy needed to quantitatively asses the different sources and sinks
- Ground-based demonstrators of the present instrument concept are under development both at Univ. of Basilicata and Univ. of Hohenheim.

carbon dioxide measurements based on the application of the Raman lidar technique have been carried out since the early nineties (Riebesell, 1990; Ansmann et al., 1992). The technique is based on the measurement of anelastically retro-diffused laser radiation (retro-diffusion Raman roto-vibrational) from the carbon dioxide molecules present in the atmosphere.

Despite its important potential scientific applications, the Raman lidar technique for the measurement of carbon dioxide has received little attention in the last 25 years both at theoretical and experimental level, mainly due to the limited precision that characterizes this measure, due to the limited section d impact of the scattering phenomenon on which the technique is based and the low concentration of the species of interest.

Misure a carattere sperimentale del contenuto atmosferico dell' anidride carbonica basate sull'impiego della tecnica lidar Raman sono state realizzate sin dai primi anni novanta (Riebesell, 1990; Ansmann *et al*., 1992). La tecnica si basa sulla misura della radiazione laser retro-diffusa anelasticamente (retro-diffusione Raman roto-vibrazionale) dalle molecole di anidride carbonica presenti in atmosfera. Nonostante le sue importanti potenziali applicazioni scientifiche, la tecnica lidar Raman per la misura dell' anidride carbonica ha ricevuto negli ultimi 25 anni poca attenzione sia a livello teorico che sperimentale, principalmente a causa della limitata precisione che caratterizza questa misura, riconducibile alla limitata sezione d'urto del fenomeno di scattering su cui la tecnica si basa ed alla bassa concentrazione della specie d'interesse.

Ad ogni modo, nell'ultimo decennio sono stati conseguiti enormi progressi nella progettazione e nello sviluppo sperimentale di sorgenti laser a stato solido con elevata potenza, di telescopi a grande apertura e di rivelatori ad elevato guadagno ed efficienza quantica, progressi che consentono di poter raggiungere oggi un nuovo livello di prestazioni nelle misure lidar Raman dell' anidride carbonica.

Per stimare le prestazioni potenziali di un sistema lidar è necessario far uso di un simulatore. A tale scopo, la precisione delle misure lidar Raman del rapporto di mescolamento dell'anidride carbonica, sia in orario diurne che notturno, è stata stimata mediante l'impiego di un simulatore sviluppato presso la Scuola di Ingegneria dell'Università della Basilicata (Di Girolamo et al., 2006). La grandezza misurata dal lidar Raman, sia nel caso del vapore acqueo (Whiteman *et al*., 1992) che della CO_2 (Ansmann *et al*. 1992), è il rapporto di mescolamento rispetto all'aria secca. Per poter quantificare questa grandezza si fa uso della misura simultanea della retrodiffusione Raman da parte dell' azoto molecolare per normalizzare il segnale Raman retro-diffuso dalle molecole di vapore acqueo o di anidride carbonica.

Le simulazioni sono state effettuate assumendo una integrazione temporale di misura (risoluzione temporale) di 1 ora ed una risoluzione verticale di 75 m sotto 1.25 km, di 150 m nella regione di quote 1.25-2.0 km, di 250 m nella regione di quote 2.0-2.5 km, di 400 m nella regione di quote 2.5-3.0 km e di 600 m sopra 3.0 km.

I dati di ingresso del modello includono un profilo del rapporto di mescolamento dell'anidride carbonica caratterizzato da un aumento di 10 ppm ad un'altezza di 2.2 km (da un valore di 350 ad uno di 360 ppm), introdotto per poter simulare la diminuzione della CO_2 che si verifica al tetto dello strato misto durante il corso del giorno. Questo profilo simula una possibile condizione poco dopo il tramonto. Il carico aerosolico è stato simulato assumendo la presenza di uno strato con un coefficiente di estinzione costante e pari a 0.05 km^{-1} nei primi 2 km di quota. Le simulazioni considerano un sistema lidar, con una sorgente laser di tipo Nd:YAG in grado di emettere una potenza ottica nell'UV (354.7 nm) di 30 W (energia di singolo impulso=3 J, frequenza di ripetizione=100 Hz) ed un telescopio per la raccolta dei segnali lidar con uno specchio primario di diametro pari a 0.6 m. Le simulazioni considerano inoltre che la selezione spettrale della banda Raman del CO_2 (Q-branch della banda Raman roto-vibrazionale u2 della CO_2, che risulta spostata rispetto alla lunghezza d'onda laser di 1285 cm^{-1}) venga effettuata mediante l'impiego di un filtro interferenziale, con le seguenti specifiche: lunghezza d'onda centrale (CWL) = 371.71 nm, larghezza spettrale di banda (BW) = 0.1 nm, trasmissione a CWL = 40%, reiezione fuori banda = OD6 @ 200-1200 nm, OD12 @ 354.7 nm e OD7 @ 375-387 nm. Le simulazioni considerano infine una altezza di volo dell'aereo ospitante il sistema lidar di 4 km.

Le simulazioni evidenziano come la diminuzione del rapporto di mescolamento della CO_2 che si verifica al tetto dello strato misto sia ben risolto utilizzando un sistema lidar Raman dimensionato come sopra. Più specificamente, utilizzando le risoluzioni temporali e verticali sopramenzionate, la precisione della misurazione risulta pari a ~ 2 ppm fino a circa 3 km di quota.

La lunghezza d'onda centrale (371,71 nm) è quasi coincidente con la ventiduesima riga spettrale della banda anti-Stokes dello spettro roto-vibrazionale dell'ossigeno molecolare, specie che rappresenta una potenziale fonte di contaminazione per la misura della CO_2. Riebesell (1990) e Ansmann *et al*. (1992) giunsero alla conclusione che le misure lidar Raman di anidride carbonica fossero difficilmente realizzabili a causa dell'impossibilità di poter stimare in modo accurato l'entità dell'interferenza da parte delle righe rotazionali dell'ossigeno molecolare. Questi autori ipotizzarono inoltre che misure lidar con precisioni dell'ordine del ppm potessero essere contaminate dall'eventuale presenza di fluorescenza generata dalle ottiche del ricevitore o dalle particelle atmosferiche. Tuttavia, queste ricerche erano state condotte utilizzando un laser ad eccimeri (miscela Xe:Cl), caratterizzato da uno spettro di emissione che si estende per circa 0.4 nm. L'emissione di radiazione laser su questo ampio spettro di lunghezze d'onda rende la separazione tra lo scattering Raman di 0_2 e CO_2 più difficile rispetto a quella realizzabile mediante l'uso di filtri interferenziali a banda stretta, quali quelli di cui si ipotizza sull'uso in questo prototipo, e di una sorgente laser del tipo Nd: YAG, con larghezza spettrale dell'impulso emesso di ~ 0.02 nm.

Come accennato in precedenza, il Q-branch dello spettro di Raman u2 della CO_2 è quasi coincidente con la ventiduesima riga anti-Stokes dello spettro roto-vibrazionale dell'ossigeno molecolare. Calcoli effettuati sulla base del valore della larghezza di banda del filtro interferenziale considerato per il sistema proposto (0.1 nm) indicano che il contributo di questa riga anti-Stokes dell'0_2 al segnale Raman della CO_2 è inferiore all'1 % (-3-4 ppm). Una opportuna modellazione della variabilità dell'intensità di questa riga rotazionale in funzione della temperatura può consentire di stimare in modo accurato l'ampiezza dell' interferenza in modo che questa possa essere sottratta dal segnale Raman dell' anidride carbonica (Whiteman *et al.*, 2001). Whiteman *et al.* (2001) hanno determinato che l'applicazione di questo approccio può consentire di ridurre a 0.3 ppm l'incertezza della misura del CO_2 causata da questa interferenza.

Nell'ambito di questo progetto si renderà necessario un accurato studio della fluorescenza generata dalle ottiche del ricevitore o dalle particelle atmosferiche. Tuttavia, misure preliminari ottenute utilizzando uno spettrometro accoppiato ad un ricevitore Raman (Whiteman *et al.*, 2001) non hanno evidenziato alcun significativo contributo della fluorescenza nella regione spettrale di pertinenza della banda Raman del CO_2, anche se la fluorescenza dovuta agli aerosol è stata osservata a lunghezze d'onda più lunghe.

Il sistema lidar progettato e sviluppato in forma prototipale nell'ambito di questo progetto sarà in grado di misurare oltre che i profili verticali del rapporto di mescolamento della CO2, anche i profili verticali del rapporto di mescolamento del vapor acqueo, della temperatura e delle proprietà ottiche del particolato atmosferico (coefficiente di backscattering ed estinzione a 355 nm).

Il segnale lidar Raman generato dalle molecole di anidride carbonica è molto più debole rispetto a quello generato dalle molecole di vapor acqueo, azoto ed ossigeno molecolare (questi ultimi due usati anche per la misura della temperatura atmosferica) e del segnale lidar elastico generato dal particolato atmosferico. Questo fa si che l'incertezza statistica che caratterizza le misure di queste ulteriori grandezze atmosferiche sia sensibilmente inferiore rispetto a quella che caratterizza la misura dell'anidride carbonica, rendendo quindi possibili misure accurate di questi parametri con tempi di integrazione molto più contenuti.

Referenze

Riebesell, M., 1990: Raman lidar for the remote sensing of the water vapor and carbon dioxide profile in the troposphere (in German). Ph.D. thesis, GKSS document 901/F/13, University of Hamburg, 127 pp.

Ansmann, A., M. Riebesell, C. Weitkamp, E. Voss, W. Lahmann, and W. Michaelis, 1992b: Combined Raman Elastic-backscatter lidar for vertical profiling of moisture, aerosol extinction, backscatter, and lidar ratio. Appl. Phys., 55B, 18-28.

Whiteman, D. N., S. H. Melfi, and R. A. Ferrara, 1992: Raman lidar system for the measurement of water vapor and aerosols in the earth's atmosphere. Appl. Opt., 31, 3068-3082.

Whiteman, D. N., G. Schwemmer, T. Berkoff, H1, Plotkln, L. Ramos-Izquierdo, and G. Pappalardo, 2001: Performance modeling of an airborne Raman water vapor lidar, Appl. Opt., 40,375-390.

atmosfera del rapporto di mescolamento dell' anidride carbonica. Nell'ambito dell'OR4 si intende altresì avviare lo sviluppo prototipale di questo sistema, nonché realizzare studi per l'ingegnerizzazione e la qualifica per volo aereo del sistema.

A tal riguardo si specifica che, nonostante le sue importanti potenziali applicazioni scientifiche la tecnica lidar Raman roto-vibrazionale per la misura dell' anidride carbonica ha ricevuto negli ultimi 25 anni poca attenzione sia a livello teorico che sperimentale, principalmente a causa della limitata precisione che questa tecnica era in grado di garantire, riconducibile alla limitata sezione d'urto del fenomeno di scattering Raman roto-vibrazionale ed alla bassa concentrazione della specie d'interesse. Nell'ultimo decennio, però, notevoli progressi sono stati conseguiti nella progettazione e sviluppo sperimentale di sorgenti laser a stato solido con elevata potenza ottica, di telescopi a grande apertura e di rivelatori ad elevato guadagno ed efficienza quantica, progressi che consentono oggi di poter raggiungere un nuovo livello di prestazioni nelle misure lidar Raman dell' anidride carbonica. Fruttando questi progressi, nell'ambito del progetto si intende verificare l'effettiva fattibilità e quindi progettare un sistema lidar basato su questa tecnica,

By exploiting these advances, the project intends to verify the actual feasibility and therefore to design a lidar system based on this technique.

Il cambiamento climatico in atto (e.g., *Working Group I Contibution to the IPCC fifth Assessement Report, Climate Change 2013, The Physical Science Basis,* http://www.ipcc.ch/report/ar5/wg1/) ed il relativo riscaldamento globale sono conseguenza di un'alterazione dell'effetto serra naturale del pianeta. L'effetto serra naturale è dominato per oltre il 75% dal vapore acqueo e per il restante 25% principalmente dalla CO_2. Mentre le attività antropiche aggiungono solo *poche gocce* al ciclo idrologico della Terra, esse hanno sostanzialmente alterato quello del carbonio: la concentrazione della CO2 in atmosfera è passata dai circa 300 ppmv degli anni '50 dello scorso secolo, agli attuali 405-410 ppmv del 2017, con un incremento annuo che sta superando la stima di 2 ppmv.

La combustione di combustibili fossili ed altre attivate umane immettono nell'atmosfera circa 40 miliardi tonnellate di CO_2 ogni anno. Le osservazioni della CO_2 e della sua concentrazione in atmosfera sono principalmente eseguite attraverso una rete globale di stazioni a terra. Le misure indicano che meno della metà della CO_2 immessa si accumula nell'atmosfera. La restante parte è evidentemente assorbita dagli oceani e dalla biosfera terrestre (e.g. Le Quere et al 2009, 2013). Sebbene la rete di monitoraggio al suolo si sia regolarmente espansa negli ultimi 50 anni, consentendo di avere un quadro accurato della variabilità superficiale della concentrazione della CO_2 a scala globale, essa non garantisce la dovuta risoluzione spaziale e temporale necessaria per analisi quantitative di sorgenti (sources) e pozzi (sinkes) ed, in ultima analisi, non è in grado di pervenire al bilancio biogenico connesso con l'attività di fotosintesi clorofilliana della vegetazione (Gross Primary Productivity o GPP).

Allo stato attuale esiste una carenza notevole in relazione alle osservazioni di come l'attività di fotosintesi clorofilliana e la respirazione della vegetazione risponde, a scala locale, all'incremento di temperatura e della CO_2, e ai crescenti periodi di siccità, come quelli verificatisi, e.g., nell'anno 2017. La GPP è direttamente connessa con la salute delle vegetazione, il suo stato di stress, ed in generale tutti quegli aspetti legati alla fenologia delle piante.

Questa problematica è di particolare rilevanza al nostro Paese, la cui superficie boschiva occupa circa il 35% del territorio con incendi e fenomeni franosi sempre più frequenti.

Our current knowledge about atmospheric CO2 concentrations and surface fluxes at regional scales over the globe comes primarily from ground-based in situ measurements of air sampling networks and tall towers (Reuter et al., Atmos. Meas. Tech., 5, 1349–1357, 2012).

These measurements are used by assimilation systems like NOAA's (National Oceanic and Atmospheric Administration) CarbonTracker (Peters et al., 2007, 2010), modeling global distributions of atmospheric CO2 mixing ratios and surface fluxes. Therefore, within this publication, we consider CT2010 (Carbon-Tracker version 2010) as current knowledge and reasonable a priori estimate for atmospheric CO2 concentrations (Reuter et al., Atmos. Meas. Tech., 5, 1349–1357, 2012. However, due to the sparseness of measurements, there are still large uncertainties especially on the surface fluxes (Stephens et al., 2007).

Coupling

Coupling between the Amazonian carbon cycle, global climate and global greenhouse gas burdens of CO2, CH4 and N2O (Gatti et al., *Tellus (2010), 62B, 581–594).*

Previous lidar measurements

A 1.6 m differential absorption Lidar (DIAL) system for measurement of vertical CO2 mixing ratio profiles was been developed. (Yasukuni Shibata et al., Sensors 2018, 18, 4064; doi:10.3390/s18114064).

CO2 vertical profiles in the 5–25 km altitude range with an accuracy of about 2 ppm based on Limb measurements

Major limitations of our present knowledge of the global distribution of CO2 in the atmosphere are the uncertainty in atmospheric transport and the sparseness of in situ concentration measurements. Limb viewing space-borne sounders such as the Atmospheric Chemistry Experiment Fourier transform spectrometer (ACE-FTS) offer a vertical resolution of a few km for profiles, which is much better than currently flying or planned nadir sounding instruments can achieve (P. Y. Foucher, Atmos. Chem. Phys., 11, 2455–2470, 2011).

Seasonal swing ranged between 20 and 35 ppm for CO_2 mixing (CHUN-TA LAI, Tellus, 58B, 523–536, 2006).

Studies about current spatial and temporal variations of CO_2 in forest canopies provide critical information about how well a forest is coupled to the convective boundary layer (CBL) above the canopy, and therefore how susceptible this ecosystem is to increased atmospheric CO_2 (Buchmann et al., Global Change Biology, **2,** 421-432, 1996).

CO_2 gradients between the forest floor and the top of the canopy ranged between 75 and 100 ppmv at night, compared to 10-50 ppmv during the day. Both ranges represented spring conditions when canopy leaf area development had not been completed (Buchmann et al., Global Change Biology, **2,** 421-432, 1996).

Despite the lack of tree foliage and understorey vegetation, it is found a 5 ppmv canopy gradient during the day, but an average 23 ppmv gradient at night. (Buchmann et al., Global Change Biology, **2,** 421-432, 1996)

During June and July, [COj] in the upper and lower canopy (3.30-14.0 m) dropped below those of the CBL, depleting canopy air by 1-2 ppmv in June, and by 4-11 ppmv in July. Lowest canopy CO2 were reached in July, before they Increased again in fall (Buchmann et al., Global Change Biology, **2,** 421-432, 1996).

	Pinus contorta	Populus Tremuloides	Red Butte Canyon Acer spp
Canopy height	13-15 m	9-13 m	13-15 m

(Buchmann et al., Global Change Biology, **2,** 421-432, 1996)

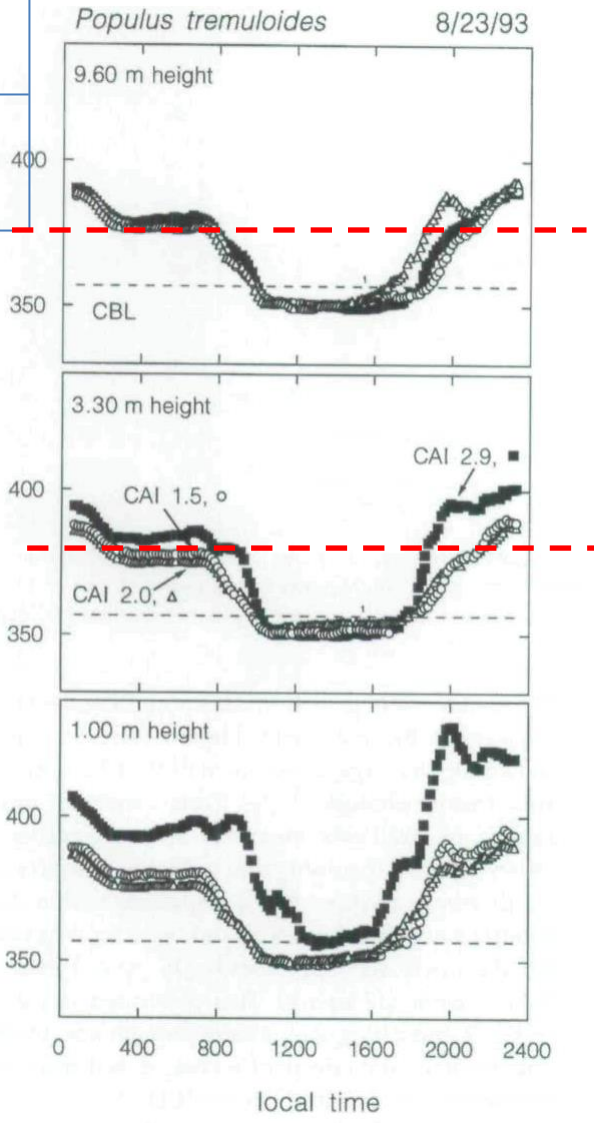

As clearly reported in the IPCC fifth Assessment Report, CO_2 emissions are already producing destructive effects to the plant ecosystem through the alteration of soil-atmosphere interaction mechanisms.

Although the space and ground network for CO_2 monitoring has regularly expanded over the past 50 years, it does not guarantee the necessary spatial and temporal resolution needed for a quantitative analysis of sources and sinks.

For the purpose of estimating forests' carbon capturing capabilities, accurate measurements of CO_2 gradients between the forest floor and the top of the canopy, which ultimately translates into the capability to measure CO_2 concentration profiles. Space sensors provide CO_2 measurements above forest canopies, which do not allow to properly estimate Gross Primary Production (GPP). These observational gaps could be addressed with an active remote sensing system in space based on the roto-vibrational Raman lidar technique. CO_2 profile measurements are possible, together with simultaneous measurements of the temperature and water vapour mixing ratio profile and a variety of additional variables (aerosol backscatter profile, aerosol extinction profile, PBL depth, cloud top and base heights, cloud optical depth). An assessment of the expected performance of the system has been performed based on the application of an analytical simulation model developed at University of Basilicata.

Space sensors provide CO_2 measurements above forest canopies, which do not allow to properly estimate the Gross Primary Production (GPP).

- The estimated amount of carbon dioxide (CO_2) in the atmosphere is equivalent to an amount of carbon of 8×10^{14} kg, while the amount stored in terrestrial biomass is 5×10^{14} kg, 60% of which (3×10^{14} kg) being stored in forest systems.

N is the number of atoms

number vibrations.

The same holds true for linear molecules, however the equations 3N-5 is used, because a linear molecule has one less rotational degrees of freedom. (For a more detailed explanation see: Normal Modes). Figure 1 shows a diagram for a vibrating diatomic molecule. The levels denoted by vibrational quantum numbers v represent the potenital energy for the harmonic (quadratic) oscillator. The transition $0 \rightarrow 1$ $0 \rightarrow 1$ is fundamental, transitions $0 \rightarrow n$ $0 \rightarrow n$ $(n>1)$ are called overtones, and transitions $1 \rightarrow n$ $1 \rightarrow n$ $(n>1)$ are called hot transitions (hot bands).

a observational requirements have to be properly assessed.

CO_2 vertical variability

The seasonal and annual mean of CO_2 vertical profile reflect the combined influences of surface fluxes and atmospheric mixing. In the Northern Hemisphere, during the summer season, midday atmospheric CO_2 concentrations are generally lower near the surface than in the free troposphere, reflecting the higher impact of terrestrial photosynthesis over industrial emissions [5]. Conversely, during the winter, respiration and fossil-fuel sources lead to elevated low-altitude atmospheric CO_2 concentrations. The gradients are comparable in magnitude in both seasons, but the positive gradients persist for a larger portion of the year, leading to annual-mean gradients also showing higher atmospheric CO_2 concentrations near the surface than aloft [5]. The average midday differences in the Northern Hemisphere between 1 and 4 km, expressed in terms of CO_2 mixing ratio, is –2.2 ppm in summer, +2.6 ppm in winter, while instantaneous differences may be as large as 5-10 % [9]. The Southern Hemisphere locations show relatively constant CO_2 profiles in all seasons, with slightly higher values in the free troposphere [5]. Similar gradients are found in the NOAA's Carbon Tracker version 2010 [4]. CO_2 gradients between the forest floor and the top of the canopy range between 75 and 100 ppm at night, compared to 10-50 ppm during the day. Both ranges represented spring conditions when canopy leaf area development is not completed [10].

The central wavelength of the CO_2 band is almost coincident with the twenty-first anti-Stokes roto-vibrational O_2 line, which represents a potential source of contamination for CO_2 Raman lidar measurements [11]. Riebesell [6] and Ansmann et al. [7] came to the conclusion that CO_2 Raman lidar measurements were hardly feasible due to the difficulties in accurately estimating the magnitude of the interference by O_2 rotational lines. These authors also argued that fluorescence generated by either the receiver optics or atmospheric particles could potentially prevent from reaching a measurement accuracy at the 1 ppm level.

However, these early research efforts were conducted using excimer laser sources (Xe:Cl mixture), which have an emission spectrum typically spanning over a spectral interval of ~0.4 nm. Such broad spectrum makes separation of CO_2 and O_2 lines more difficult with respect to what is presently achievable based on the use of narrowband interference filters (0.1 nm) and injection-seeded Nd:YAG laser sources (typical spectral width of ~0.01 nm). Whiteman et al. [11] demonstrated that the bias affecting CO_2 measurements as a result of the contamination by the 21st O_2 rotational line is not exceeding 1 % if a 0.1-nm wide IF and a narrow-band Nd:YAG laser source (<0.02 nm) are used. Based on an appropriate rotational strength modeling as a function of temperature and relying on independent temperature profile measurements provided by the same Raman lidar system, the magnitude of the interference can be properly estimated and subtracted from the CO_2 signal so that a residual systematic uncertainty of the order of 0.1-0.2 ppm is left in CO_2 mixing ratio measurements.

Observational requirements for CO_2 profiling - continuation

The average Northern Hemisphere midday differences between altitudes of 1 and 4 km is –2.2 ppm in summer, +2.6 ppm in winter, and +0.7 ppm in annual mean.

The Southern Hemisphere locations show relatively constant CO_2 profiles in all seasons, with slightly higher values in the free troposphere.

Similar gradients are found in the NOAA's (National Oceanic and Atmospheric Administration) Carbon Tracker version 2010 (CT2010).

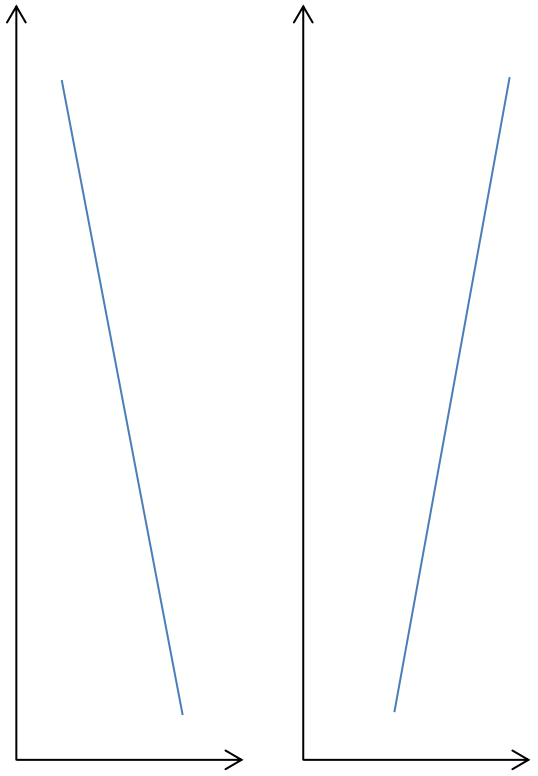

An assessment of the expected performance of the system has been performed based on the application of an analytical simulation model developed at University of Basilicata.

Fermi resonance results in the splitting of two vibrational bands that have nearly the same energy and symmetry in both IR and Raman spectroscopies. The two bands are usually a fundamental vibration and either an overtone or combination band.

As a result, two strong bands are observed in the spectrum, instead of the expected strong and weak bands. It is not possible to determine the contribution from each vibration because of the resulting mixed wave function.

Sistema lidar Raman per la misura dei profili verticali in atmosfera del rapporto di mescolamento dell' anidride carbonica

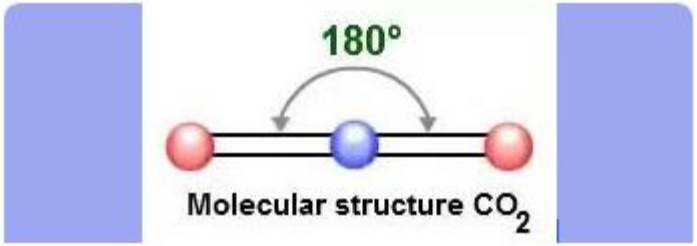

For linear molecules, however the equation 3N-5 is used, because a linear molecule has one less rotational degrees of freedom.

The *Q* branches of the Raman bands associated to the $2\nu_1:4\nu^0_2:\nu_1+2\nu^0_2$ Fermi resonance of $^{12}C\ ^{16}O_2$ have been observed in the gas phase at 2543, 2671, and 2797 cm^{-1} and, in addition, at 2514 cm^{-1},

- Alternative option: Alexandrite laser source ($BeAl_2O_4$ doped with active chromium ions, Cr^{3+})
- Main advantages:
  - ➢increase of laser gain with temperature which considerable simplifies laser cooling demands.
  - ➢Tuneability between 730-780 nm so that desired wavelength can be reached by frequency-doubling (2-times larger efficiency than frequency-tripling)
  - ➢pumped by diode lasers operating in the 500-650-nm region which are now commercially available with high power.

Although the space and ground network for CO_2 monitoring has regularly expanded over the past 50 years, it does not guarantee the necessary spatial and temporal resolution needed for quantitative analysis of sources and sinks.

- The missing balance between the carbon released in the atmosphere through the combustion of fossil fuels and deforestation on one side, and the uptake by sinks in oceanic and terrestrial systems on the other side is responsible for the 2 ppm increasing rate in atmospheric CO_2 concentration.

A proper definition of the CO_2 observational requirements impose the assessment of CO_2 time and space (vertical and horizontal) varibility

to ultimately define:

- vertical and horizontal resolution of measurements,
- measurement precision (RMS) and accuracy (bias)

but the positive gradients persist for a greater portion of the year and the annual-mean gradients also show higher atmospheric CO_2 concentrations near the surface than aloft (Stephens et al., 2007),

, with the only exception of the **vertical region from the forest floor to the top of the canopy** where uncertainty is **7 %** (or **25 ppm**) and **135 %** (or **470 ppm**), respectively

The three fundamental vibrations of CO_2 are v_1= 1337 cm^{-1}, v_2=667 cm^{-1}, v_3=2349 cm^{-1}.